Case Report

Tuberculous Scar Tumour Detected by Dual Tracer Positron Emission-Computerised Tomography in a Tuberculous Endemic Area

Chee-Kin Hui[1,2]

Submitted: 27 Jan 2014
Accepted: 8 Jun 2014

[1] *Centre for Alimentary Studies, Hong Kong SAR, China*

[2] *Quality Healthcare Medical Services, Rm 601-605, HK Pacific Centre, 28 Hankow Road, Tsim Sha Tsui, Hong Kong SAR, China*

Abstract

Tuberculous scar tumour is difficult to diagnose as it does not present with any respiratory symptoms and has a negative chest X-ray. This is a case report on the use of dual tracer ^{11}C-acetate and ^{18}F-fluorodeoxyglucose (^{18}FDG) whole body positron emission tomography-computerised tomography (PET-CT) for detection of tuberculous scar tumour. A 44-year-old Chinese female was incidentally found to have a raised serum Ca 19.9. Magnetic resonance imaging of the whole abdomen, upper endoscopy, and colonoscopy were all unremarkable. A low-dose computed tomography (CT) of the thorax showed bilateral upper lobe fibrosis. Bronchoalveolar lavage for culture and cytology was negative. A dual tracer ^{11}C-acetate and ^{18}FDG whole body PET-CT showed that the left upper lobe fibrosis was hypermetabolic in nature. It was more avid for ^{11}C-acetate than for ^{18}FDG. The left upper lobe lesion was subsequently confirmed on open lung biopsy to be a moderately differentiated adenocarcinoma. Therefore, in a tuberculous endemic region, dual tracer whole body PET-CT with ^{11}C-acetate and ^{18}FDG may have a role in the early detection of tuberculous scar tumour in the lung.

Keywords: *Scar tumour, positron emission tomography-computerized tomography, ^{11}C-acetate, F-18 Fluorodeoxyglucose*

Introduction

Tuberculous scar tumour was first described more than 50 years ago (1). It is usually an adenocarcinoma, with a predilection for early metastasis and is located in the periphery of the upper lobes of the lungs (1). Unfortunately, it usually does not present with any respiratory symptoms and has a negative chest X-ray. These factors may contribute to the poorer prognosis associated with tuberculous scar tumour (2). This is the first reported case on the use of dual tracer ^{11}C-acetate and ^{18}F- fluorodeoxyglucose (^{18}FDG) whole body positron emission tomography-computerized tomography (PET-CT) to detect tuberculous scar tumour in a tuberculous endemic region.

Case Report

A 44-year-old Chinese female was incidentally found to have a raised serum carbohydrate antigen (Ca) 19.9 of 53.3 U/mL (normal range ≤ 37 U/mL) (Figure 1). She was asymptomatic and was a non-smoker. Her only significant past medical history was sputum culture positive pulmonary tuberculosis diagnosed at the age of 28. Clinical examination on presentation was unremarkable. In order to search for an abdominal cause for the raised serum Ca 19.9; especially a pancreatic lesion; magnetic resonance imaging (MRI) (plain and contrast] of the abdomen and pelvis was performed. The MRI of the abdomen and pelvis) was performed with a 1.5-T whole-body imager (Signa LX; General Electric Medical Systems, Milwaukee, WI, USA). All MRI images were acquired in the axial plane with a phased-array body multicoil. The slice thickness was 7 mm, with a 0.7 mm intersection gap for all of the pulse sequences. Fat-suppressed T2-weighted imaging was obtained with a respiratory-triggered fast spin-echo sequence (4000 to 8000/102): effective relaxation time (TR)/effective excitation time (TE), 16 echo train length, four signals acquired, 10-millisecond interecho spacing, 320 × 224 matrix, 31.25 kHz received bandwidth, 280 to 400 mm field of view, 30% respiratory trigger point, 40% trigger window, and gradient moment nulling in the frequency-encoding direction. Saturation bands above and below the imaging volume were used to attenuate flow-related artefacts throughout the MRI. Breath-hold single-shot fast spin-echo sequences were obtained using the following parameters:

minimum/90 (effective TR/effective TE), half-Fourier acquisition, 104 echo train length, one signal acquired, 320 × 224 matrix, 62.5 kHz received bandwidth, and 40 cm field of view. Dynamic contrast-enhanced MRI images were obtained with an initial delay of 16 seconds for the arterial phase, a 50–second delay for the venous phase, and 2 minutes and 5 minutes after the initiation of a bolus injection of 0.1 mmol/kg of Gd-DOTA (Dotarem, Guerbet, France) into the antecubital vein. Three-dimensional (3D) LAVA mode, T1-weighted sequences were acquired with fast multiplanar spoiled gradient-recalled echo imaging (125/4.2) TR/TE, 60-degree flip angle, one signal acquired, 320 × 192 matrix, 62.5 kHz received bandwidth, slice thickness 4.4 mm, 40 cm field of view, and 25 seconds acquisition time in a single breath-hold.

There was no evidence of tumour in the abdomen and pelvis on MRI. The patient then proceeded to undergo upper endoscopy and colonoscopy to look for a possible site of a Ca 19.9 producing tumour. These both were also unremarkable.

Although her chest X-ray was unremarkable, a screening low dose computed tomography (CT) of the thorax was performed to look for possible lung lesion that may account for her raised serum Ca 19.9 since all of her work-up to this point was unremarkable. The low dose CT of the thorax showed fibrocalcific changes involving both the left and right upper lobes. There was no evidence of consolidation or cavitation to suggest reactivation of tuberculosis. There was no radiological feature to suggest the presence of a tiny neoplastic lesion in these two fibrocalcific lesions (Figure 2a, 2b). Her Quantiferon® TB Gold In-tube test (Cellestis Inc., Valencia, CA, USA) was positive at 3.43 IU/mL (normal range < 0.35 IU/mL) but her tuberculin skin test was negative.

Because of the findings of the thorax on CT, coupled with the positive Quantiferon® TB Gold test and raised serum Ca 19.9, a fibreoptic bronchoscopy was performed. Bronchoalveolar lavage was performed for bacterial culture, fungal culture, acid fast bacilli (AFB) smear, AFB culture and *Mycobacteria tuberculosis* polymerase chain reaction, which were all negative. Bronchoalveolar lavage for cytology was also negative for malignant cells.

As all investigation was negative for malignancy, we decided to serially monitor the patient's serum Ca 19.9 (Figure 1). Although she remained well and asymptomatic, a dual tracer 11C-acetate and 18FDG whole body PET-CT was performed seven months after presentation, as her serum Ca 19.9 was on an increasing trend (Figure 1).

For the dual tracer whole body PET-CT, the 11C-acetate (440–590 MBq; 7.4 MBq/kg of body weight) was administered intravenously. Limited whole body (from base of skull to upper thighs) imaging was performed 20 minutes after injection. Data acquisition was obtained using an integrated in-line PET-CT scanner (Biograph 16 lutetium oxyorthosilicate HI-REZ, Siemens Medical Solutions, Knoxville, TN, USA) beginning with a CT (without contrast, 130 kV, 110-115 mA, 2 mm pitch and 1s tube rotation). The CT was followed by PET with a 2 mm emission acquisition time and a 16.2 cm axial field of view per position. The 330–520 MBq (6.3 MBq/kg of body weight) ^{18}FDG was injected intravenously

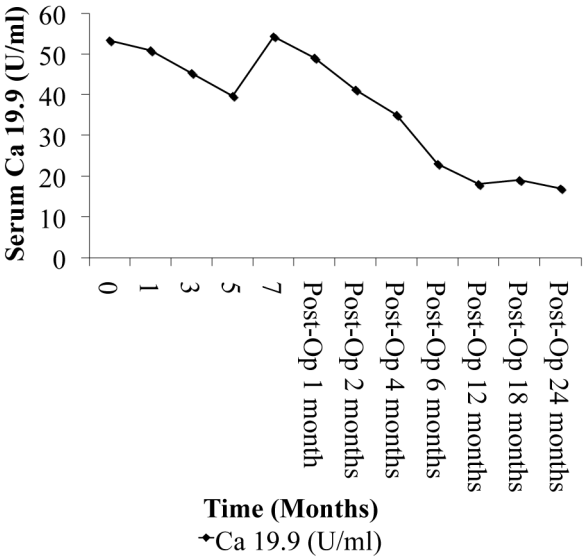

Figure 1: Graph showing serial serum carbohydrate antigen 19.9.

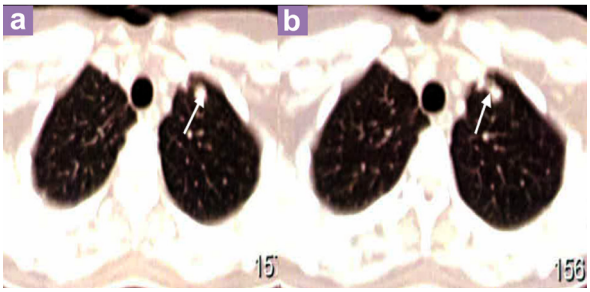

Figure 2: (a, b) Computerised tomography of the thorax showing the benign looking fibrocalcific lesion in the left upper lobe.

15 minutes after completion of ^{11}C-acetate imaging. PET-CT imaging was performed 60 minutes after ^{18}FDG administration at the same positions and acquisition settings. A lesion was regarded as positive for either ^{11}C-acetate or ^{18}FDG based on visual judgement of the degree of increased metabolism, supported by calculation of the standardised uptake value (SUV). A lesion was considered negative for ^{11}C-acetate or ^{18}FDG if it was isointense with non-tumourous tissue on visual inspection, and, supported by a lesion-to-liver SUV ratio of less than 1.20. Both the maximum and average values were calculated. The region of interest (ROI) was drawn automatically at a 75% threshold of the maximum lesion count of the tumour. The same ROI was used to evaluate the SUV of normal liver tissue.

On dual tracer whole body PET-CT, a hypermetabolic ill-defined lung nodule was identified in the apicoposterior segment of the left upper lobe. This lesion seemed to be tethered to the adjacent left brachiocephalic vein. It measured 0.8 cm by 1.9 cm in size and was more avid for ^{11}C-acetate avid than for ^{18}FDG. The SUVmax of ^{11}C-acetate was 10.3.

Figure 3a shows that the left apical lung lesion was more 11C-acetate avid when compared with the normal liver tissue (Figure 3b) and with blood pool activity within the mediastinal great vessel (descending aorta) (Figure 3c). Figure 4a and figure 4b show the maximum-intensity-projection positron emission images for the ^{11}C-acetate avid lesion. The SUVmax for ^{18}FDG at this site was only 1.6.

On the other hand, the right upper lobe fibrosis had no abnormal ^{11}C-acetate uptake. It did, however, have mild ^{18}FDG uptake with a SUVmax of 1.8.

In view of the PET-CT finding of the 11C-acetate avid lesion in the left upper lobe and the rising Ca 19.9 level, an open lung biopsy of the left upper lobe lesion for frozen section was performed. The frozen section showed evidence of carcinoma, and, the patient then underwent left upper lobe lobectomy.

On histology, the lobectomy specimen showed a moderately differentiated adenocarcinoma; 1.2 cm in size. The tumour was subpleural with no penetration of the pleural surface. The bronchial and vascular margins were clear of tumour. The bronchial lymph nodes, inferior ligament lymph nodes and aorto-pulmonary (AP) window lymph nodes were also free of tumour. The remaining lung tissue contained foci of mild interstitial fibrosis, chronic inflammation and reactive atypical cells. Therefore, the patient had stage IA cancer of the lung.

The patient's serum Ca 19.9 normalised four months after lobectomy (Figure 1). She was followed-up for 24 months post-lobectomy and no increase in serum Ca 19.9 was detected (Figure 1). Repeat dual tracer whole body PET-CTs at 6 months, 12 months, and 24 months post-lobectomy revealed no abnormal ^{11}C-acetate avid lesion. The right upper lobe lesion remained unchanged for both ^{11}C-acetate and ^{18}FDG post-operatively.

Discussion

Pulmonary tuberculosis increases the risk of primary lung tumour by causing substantial

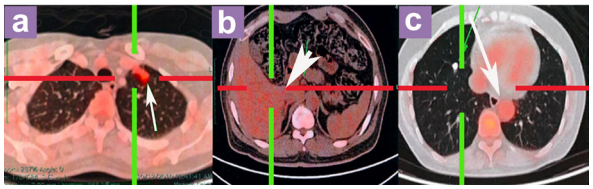

Figure 3: (a) ^{11}C-acetate avid lesion in the left upper lobe on positron emission tomography-computerised tomography; compared with the; (b) ^{11}C-acetate uptake in the normal liver; and; (c) ^{11}C-acetate uptake in the blood pool activity within the mediastinal great vessel (descending aorta).

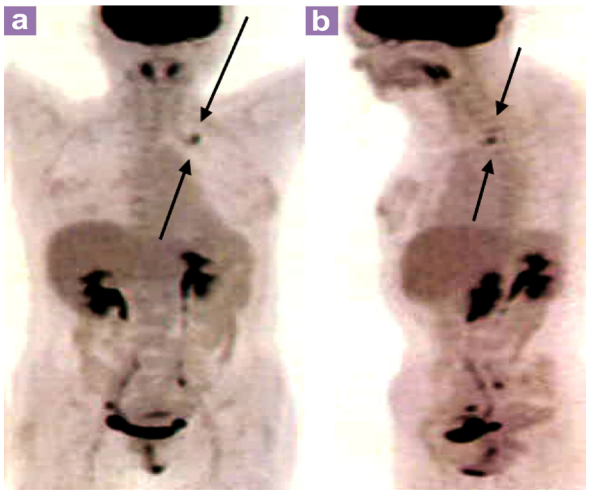

Figure 4: (a, b) The maximum-intensity-projection positron emission images for the ^{11}C-acetate avid lesion.

pulmonary inflammation, which is conducive to carcinogenesis. (3,4). The scarring process may also lead to an earlier blockage of the lymphatic system (5). This accumulation of carcinogens inside the scar for an extended period of time may cause extensive vascular and lymphatic seeding, thereby, accounting for the poor prognosis associated with tuberculous scar tumour.

However, if we were able to diagnose tuberculous scar tumour earlier, we may, theoretically, be able to improve its' prognosis. This hypothesis was given credence when Bakris et al., found that their cases of scar tumour diagnosed incidentally on post-mortem examination showed no evidence of metastasis (2).

However, tuberculous scar tumour is difficult to diagnose as it usually shows no abnormality on chest X-ray and has no pulmonary symptoms (2,5). CT of the thorax would usually show lung fibrosis, as in this case. Even PET-CT with 18FDG alone cannot be reliably used to differentiate malignancy from benign lesions; especially in a tuberculous endemic area (6,7).

Therefore, a dual tracer ^{11}C-acetate and ^{18}FDG whole body PET-CT was performed on this patient. As tuberculous scar tumour is usually a well-differentiated or well-to-moderately differentiated tumour (1,2), it will preferentially accumulate ^{11}C-acetate and will tend to be negative for ^{18}FDG (8–12). The ^{11}C-acetate would, theoretically, complement the ^{18}FDG as it does in primary hepatocellular carcinoma, urologic tumours and hemangiopericytoma (8–12). Tuberculoma, which can have enhanced ^{18}FDG (6,7), should not be 11C-acetate avid. The dual tracer PET-CT should allow us to differentiate and determine if a tumour has formed in the fibrotic lesions in the upper lobes in this case.

The early stage of tumour (stage IA) discovered in this patient and its remission 24 months after lobectomy supports the postulation that the prognosis of scar tumour may be improved with early diagnosis (2,3,5). Dual tracer ^{11}C-acetate and ^{18}FDG whole body PET-CT may provide clinicians with a more sensitive and specific tool for detecting tuberculous scar tumour, especially in a tuberculous endemic region. To my knowledge, this is the first case report documenting the use of dual tracer ^{11}C-acetate and ^{18}FDG whole body PET-CT for detecting tuberculous scar tumour.

On another note, serum Ca 19.9 was initially identified in 1979 (13). It was first described in colorectal cancer cell lines by Koprowski et al., with the use of a monoclonal antibody known as 1116-NS-19-9 (14). Serum Ca 19.9 was subsequently identified in pancreatic tumours, oesophageal tumours, gastric tumours, and biliary tumours (14). Since then, it has also been discovered to be raised in respiratory diseases (14). Whether the raised serum Ca 19.9 was produced by the tuberculous scar tumour in our case cannot be confirmed.

The raised Ca 19.9 in this patient may have been a coincidence. However, as her serum Ca 19.9 normalised post-lobectomy, this does provide a basis to suspect its elevation was caused by the tuberculous scar tumour. This hypothesis would be strengthened if the tumour had been stained for Ca 19.9. Unfortunately, this was not performed.

Conclusion

In conclusion, in a tuberculous endemic region, dual tracer whole body PET-CT with ^{11}C-acetate and ^{18}FDG may have a role in the detection of tuberculous scar tumour in the lung. Further studies on the use of dual tracer whole body PET-CT with ^{11}C-acetate and ^{18}FDG for diagnosis of pulmonary lesions in a tuberculous endemic region should be conducted in order to determine its' efficacy.

Acknowledgement

Thank you to Dr A Lim; United Kingdom for providing the PET-CT images; Dr Kui-Fai Chan; Hong Kong for providing the MRI protocol and sequence.

Conflict of Interest

None.

Funds

None.

Correspondence

Dr Chee-Kin Hui
MD (HK), MBBS (HK), MRCP (UK), FHKCP, FHKAM (Medicine)
601 HK Pacific Centre
28 Hankow Road
Tsim Sha Tsui
Hong Kong SAR
China
Tel: +852 27231183
Fax: +852 27236620
Email: bckhui@gmail.com

References

1. Yokoo H, Suckow E. Peripheral lung cancers arising in scars. *Cancer*. 1961;**14**:1205–1215.

2. Barkis GL, Mulopulos GP, Korchik R, Ezdinli EZ, Ro J, Yoon BH. Pulmonary scar carcinoma: a clinicopathologic analysis. *Cancer*. 1983;**52(3)**:493-497.

3. Wu CY, Hu HY, Pu CY, Huang N, Shen HC, Li CP, Chou YJ. Pulmonary tuberculosis increases the risk of lung cancer. *Cancer*. 2011;**117**:618–624.

4. Nalbandian A, Yan BS, Pichugin A, Bronson RT, Kramnik I. Lung carcinogenesis induced by chronic tuberculosis infection: the experimental model and genetic control. *Oncogene*. 2009;**28(17)**:1928-1938. doi: 10.1038/onc.2009.32.

5. Carroll R. Influence of scars on primary lung cancer. *J Pathol Bacteriol*. 1962;**83**:293-297.

6. Liao CY, Chen JH, Liang JA, Yeh JJ, Kao CH. Meta-analysis study of lymph node staging by 18 F-FDG PET/CT scan in non-small cell lung cancer: comparison of TB and non-TB endemic regions. *Eur J Radiol*. 2012;**81(11)**:3518–3523. doi: 10.1016/j.ejrad.2012.02.007.

7. Sathekge MM, Maes A, Pottel H, Stoltz A, van de Wiele S. Dual time point FDG PET/CT for differentiating benign from malignant solitary pulmonary nodules in a TB endemic area. *S Afr Med J*. 2010;**10(9)**:598–601.

8. Park JW, Kim JH, Kim SK, Kang KW, Park KW, Choi JI, et al. A prospective evaluation of 18F-FDG and 11C-acetate PET/CT for detection of primary and metastatic hepatocellular carcinoma. *J Nucl Med*. 2008;**49(12)**:1912–1921. doi: 10.2967/jnumed.108.055087.

9. Oyama N, Akino H, Suzuki Y, Kanamaru H, Miwa Y, Tsuka H, et. al. Prognostic value of 2-deoxy-2-[F-18] fluoro-D-glucose positron emission tomography imaging for patients with prostate cancer. *Mol Imaging Biol*. 2002;**4(1)**:99-104.

10. Shreve P, Chiao PC, Humes HD, Schwaiger M, Gross MD. Carbon-11-acetate PET imaging in renal disease. *J Nucl Med*. 1995;**36(9)**:1595–1601.

11. Jong I, Chen S, Leung YL, Cheung SK, Ho CL. 11C-Acetate PET/CT in a Case of Recurrent Hemangiopericytoma. *Clin Nucl Med*. 2014;**39(5)**:478–479. doi: 10.1097/RLU.0b013e31829af8e3.

12. Lin C, Ho CL, Ng SH, Wang PN, Huang Y, Lin YC, et. al. (11)C-acetate as a new biomarker for PET/CT in patients with multiple myeloma: initial staging and postinduction response assessment. *Eur J Nucl Med Mol Imaging*. 2014;**41(1)**:41–49. doi: 10.1007/s00259-013-2520-x.

13. Koprowski H, Steplewski Z, Mitchell K, Herlyn M, Herlyn D, Fuhrer P. Colorectal carcinoma antigens detected by hybridoma antibodies. *Somat Cell Genet*. 1979;**5(6)**:957–972.

14. Duffy MJ, Sturgeon C, Lamerz R, Haglund C, Holubec VL, Klapdor R, et. al. Tumor markers in pancreatic cancer: a European Group on Tumor Markers (EGTM) status report. *Ann Oncol*. 2010;**21(3)**:441–447. doi: 10.1093/annonc/mdp332.